Compliant parallel robot with 6 DOF

Jürgen Hesselbach and Annika Raatz*
Institute of Machine Tools and Production Technology
Technical University Braunschweig, Germany

ABSTRACT

In this paper a patented parallel structure[1] will be presented in which conventional bearings are replaced by flexure hinges made of pseudo-elastic shape memory alloy. The robot has six degrees of freedom and was developed for micro assembly tasks. Laboratory tests made with the robot using conventional bearings have shown that the repeatability was only a couple of 1/100 mm instead of the theoretical resolution of the platform of < 1 µm. Especially the slip-stick effects of the bearings decreased the positional accuracy. Because flexure hinges gain their mobility only by a deformation of matter, no backlash, friction and slip-stick-effects exist in flexure hinges. For this reason the repeatability of robots can be increased by using flexure hinges. Joints with different degrees of freedom had to be replaced in the structure. This has been done by a combination of flexure hinges with one rotational degree of freedom. FEM simulations for different designs of the hinges have been made to calculate the possible maximal angular deflections. The assumed maximal deflection of 20° of the hinges restricts the workspace of the robot to 28x28 mm with no additional rotation of the working platform. The deviations between the kinematic behavior of the compliant parallel mechanism and its rigid body model can be simulated with the FEM.

Keywords: compliant mechanism, parallel structure, flexure hinges, pseudo-elastic single crystal CuAlNiFe, micro assembly, high precision robots

1. INTRODUCTION

An emerging field of production automation is the field of high precision applications in micro assembly. The increasing complexity of micro mechanical systems, such as sensor arrays or actuators, leads to non-monolithic systems on account of technical or economical reasons. Even though some market surveys predict a high potential for these products the number of applications is still limited. Restraints are mainly seen in the production technology which does not fit the demands of these miniaturized components.[2] Missing are new adapted handling devices for the production of micro-systems themselves and the connection of the systems to the macro world, which always require some kind of assembly. Principal demands on the device technique result from the high required accuracies, size reduction, flexibility and clean room conditions. In various works different handling devices, e.g. robots, grippers, transfer systems, have been developed which fulfil these requirements.[3-9] The overall dimensions of these devices are mostly adapted to the size of the objects to be handled. The miniaturization of the handling devices themselves has various advantages, e.g. the dynamics of small systems are better due to scaling effects; inaccuracies due to thermal expansions are reduced; active forces are fitted to needed gripping and joining forces.

As an alternative to conventional serial robots parallel robots can be used. Due to their mechanical structure parallel robots have advantages with respect to speed and positioning accuracy. Compared to serial robots the miniaturization of a parallel structures is much easier because all joints are passive. Due to the passive joints the integration of flexure hinges in parallel robots is rather simple and has already been realized in various positioning systems.[10-12] The ability to install all drives fixed to the frame makes them also suitable for handling operations under clean room conditions.

2. PARALLEL ROBOT WITH 6 DOF

2.1 Conventional parallel robot

In most of the typical assembly tasks, especially in macro assembly, only robots with four degrees of freedom are needed. In micro assembly, with very sensitive micro parts and a demand for a very high positioning accuracy, some cases require more degrees of freedom (DOF) due to alignment errors which have to be compensated by the handling

* a.raatz@tu-bs.de; phone +495313917156; fax +495313915842; http://www.iwf.ing.tu-bs.de; Institute of Machine Tools and Production Technology; Langer Kamp19b, 38106 Braunschweig, Germany

Microrobotics and Microassembly III, Bradley J. Nelson, Jean-Marc Breguet, Editors,
Proceedings of SPIE Vol. 4568 (2001) © 2001 SPIE · 0277-786X/01/$15.00

device. One example is the assembly of fiber optics with at least five degrees of freedom. For this reason a hybrid-parallel robot with six degrees of freedom has been developed at the Institute of Machine Tools and Production Technology (IWF) (fig. 1a).[13,14] The robot is driven by six linear stick slip actuators based on piezo electric actuators which are all fixed to the frame. The actuators have a smallest step size of 5nm and the incremental encoders have a resolution of 0.1 µm. Due to this and optimized geometric parameters of the structure the robot should have an accuracy in sub-µ range in a workspace of 20x20x10 mm^3. Measurements lead to a much worse repeatability with an insufficient reproducibility. One reason are the high number of joints with their backlash and slip-stick effects (fig.1b). Especially the ball joints connecting the links to the platform are poorly adjustable. If the ball joints are highly preloaded the maximum driving forces of the piezo actuators are not able to overcome the static friction of the joints. On the other hand a low preloading will result in a high backlash in the joints.

One possibility to increase the repeatability of the robot is the substitution of the conventional joints by flexure hinges. Because flexure hinges gain their mobility exclusively by a deformation of matter they are backlash-free and have no slip-stick effects. Additionally they have no abrasion. This is extremely useful when the assembly process needs clean room conditions.

Since the geometric parameters of the structure have been optimized to maximize the possible orientations of the platform in a large workspace the main geometric parameters should be obtained in the compliant structure as well. In addition this allows a comparison between the two robots, showing the influence of the integration of flexure hinges in the structure.

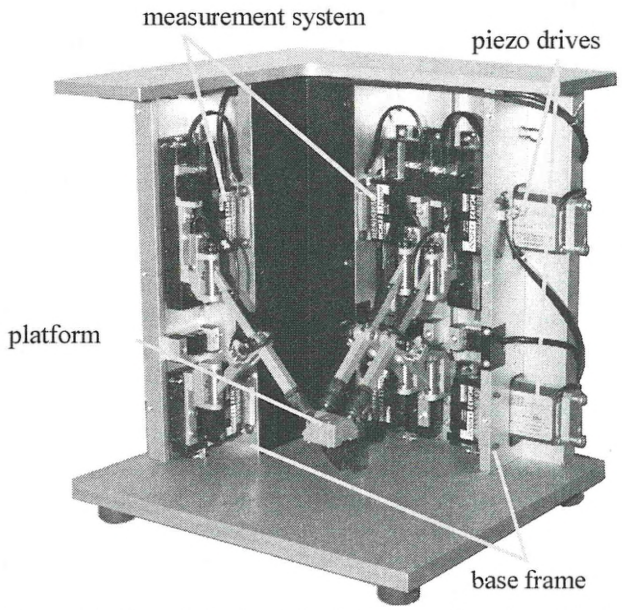

Fig. 1a: Hybrid parallel robot with six degrees of freedom (micabo[h])

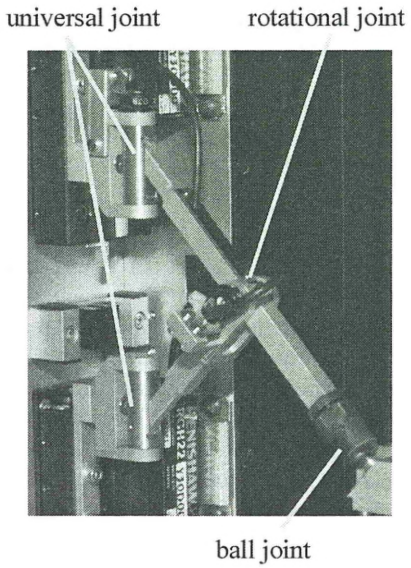

1b: Conventional joints in one chain

2.2 Kinematic of the structure

The working platform of the structure is connected by three plane sub chains with six linear actuators (fig. 2a). Since in each case two actuators have an identical linear axis (T_i) and are connected by the same link to the platform, the structure is called hybrid parallel (Fig. 2b). The drives (points B_i , B_{i+1}) are described by generalized coordinates q_i (i=1...6) and the tool center point P (TCP) by six generalized coordinates $\underline{r}_P = (X_P, Y_P, Z_P, \Psi_P, \theta_P, \varphi_P)$. Forming the rotation matrix D_{Kardan} with the angles Ψ_P, θ_P, φ_P the orientation of the platform can be described with respect to the global coordinate system XYZ.

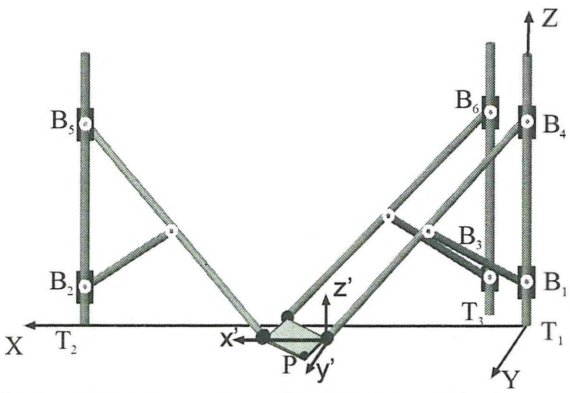

Fig. 2a: Kinematic structure of the hybrid parallel robot

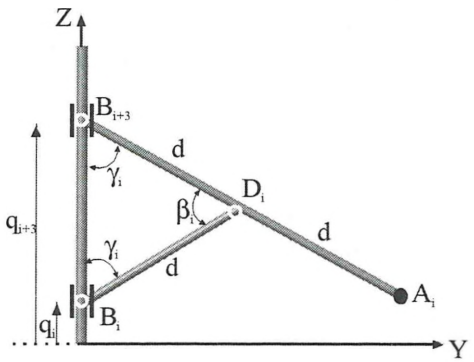

Fig. 2b: Single plane sub chain

Due to the fact that the link lengths $B_iD_i = B_{i+3}D_i = D_iA_i = d$ are the same the structure has a special kinematic behavior. The structure decouples movements in the XY-plane from vertical movements and orientations in space: the Z-coordinates of the ball joints A_i are determined only by the lower drives q_i. Due to this the inclination of the platform, that means the angles θ_P , φ_P , depends only on the coordinates of lower drives, whereas the difference between the upper and the lower drives $(q_{i+3} - q_i)$ determines the position of the tool center point in the XY-plane (X_P, Y_P) and the orientation about the Z-axis (Ψ_P). By moving the upper and lower drives equally the platform performs a movement in Z-direction.

The nonlinear interdependencies between the coordinates of the TCP and the coordinates of the drives can be expressed by an vector equation

$$\mathbf{F}(\mathbf{x}, \mathbf{q}) = \mathbf{0}. \tag{1}$$

The closure equations for the structure are (i=1...3)

$$F_{i+3}[q_i, q_{i+3}, X_{Ai}(X_P, \Psi_P, \theta_P, \varphi_P), Y_{Ai}(Y_P, \Psi_P, \theta_P, \varphi_P), Z_{Ai}(Z_P, \Psi_P, \theta_P, \varphi_P)]$$
$$\equiv (X_{Ai} - X_{Bi})^2 + (Y_{Ai} - Y_{Bi})^2 + (q_i - q_{i+3})^2 - (2*d)^2 = 0. \tag{2}$$

and for the lower drives these equations reduces to

$$F_i[q_i, Z_{Ai}(Z_P, \theta_P, \varphi_P)] \equiv Z_{Ai} - q_i = 0. \tag{3}$$

These equations can be solved by transforming the coordinates of the ball joints A_i from the platform coordinates system x'y'z' into the global coordinate system XYZ

$$\begin{pmatrix} X_{Ai} \\ Y_{Ai} \\ Z_{Ai} \end{pmatrix} = \begin{pmatrix} X_P \\ Y_P \\ Z_P \end{pmatrix} + D_{Kardan} \begin{pmatrix} x'_{Ai} - x'_P \\ y'_{Ai} - y'_P \\ z'_{Ai} - z'_{Ai} \end{pmatrix}, \tag{4}$$

leading to the solution for the inverse kinematic problem (IKP)

$$q_i = Z_{Ai} \tag{5}$$

$$q_{i+3} = q_i + ((2*d)^2 - (X_{Ai} - X_{Bi})^2 - (Y_{Ai} - Y_{Bi}))^{1/2}. \tag{6}$$

These equations are used for a comparison of the kinematic behavior of the parallel robot with conventional joints and the compliant structure.

3. COMPLIANT PARALLEL STRUCTURE

3.1 Flexure hinges

The structure contains joints with one, two and three degrees of freedom. The mostly used flexure hinges are notch hinges with one rotational degree of freedom (fig. 3). At notch hinges the deformation takes place nearly only at the point of smallest cross section (fig. 4b). To achieve high life cycles of the hinges the deformation and the strain

respectively should remain in the elastic part. In order not to restrict the mobility of the hinges and the whole structure pseudo-elastic shape memory alloys have been used as material for the hinges. The used material is a single crystal CuAlNiFe shape memory alloy with pseudo-elastic strain rates up to 17%.

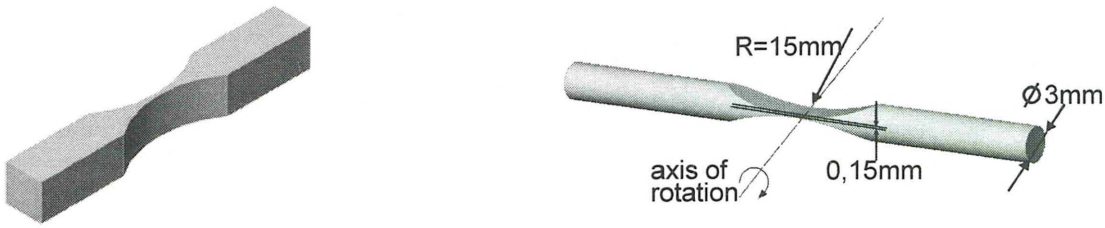

Fig. 3: Flexure hinges with circular notches and one rotational degree of freedom

Since this material is by now only available in rods with 3mm in diameter the possible geometry of the hinges is constricted (fig. 6a-d). Simulations of hinges with different geometric parameters have been made using the FEM program ANSYS. The material behavior is described by the material model MELA, where the loading path of the stress-strain-curve can be copied via the input of single stress-strain points (fig. 4a).[15]

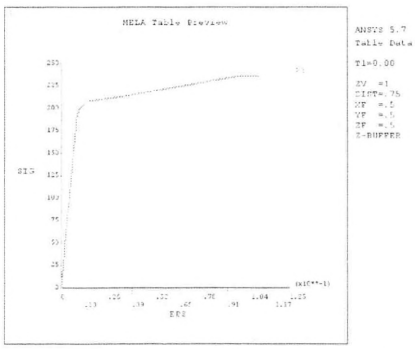

Fig. 4a: Material model MELA describing pseudo-elastic sma

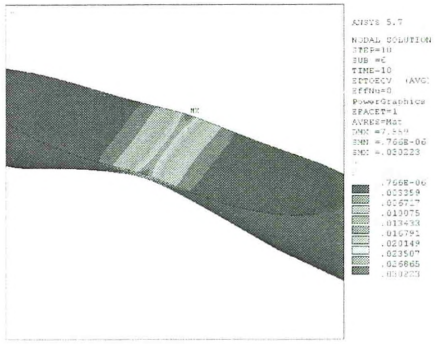

Fig. 4b: FEM simulation of sma flexure hinges

As an example of the results Fig. 5 shows the deflection angles versus the maximum strain in the hinges. As a compromise between long life cycles and a high angular deflection we chose a width of 0.15mm for the parameter t, which is the thickness of the smallest cross section, and a radius of the notch R=15mm. With these parameters the maximum strains are ε=2,6% at an angle of 20°.

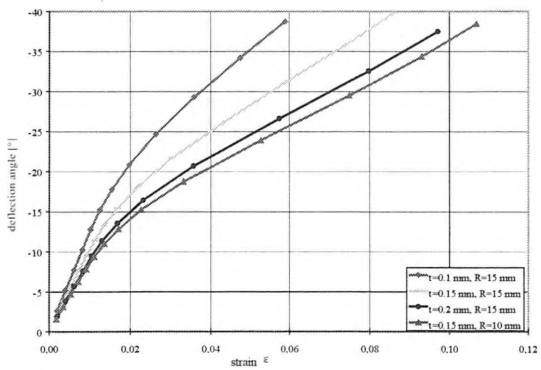

Fig. 5: Example of the maximum strains in flexure hinges versus the angular deflection varying geometric parameters

The figures 6a-d are showing possible geometries of flexure hinges with different degrees of freedom. The hinge in figure 6a has two notches which are perpendicular to each other. This allows rotations about two axes. The hinge in fig. 6b has a notch which is rotationally symmetrical, allowing arbitrary rotations and limited torsional movements. This

hinge represents a ball joint most likely. The problem with these geometries is, that with t=0.15mm the geometrical moment of inertia and the cross sectional area are very small. Due to this even only small forces would easily lead to unintentional rotations or buckling of the hinges.

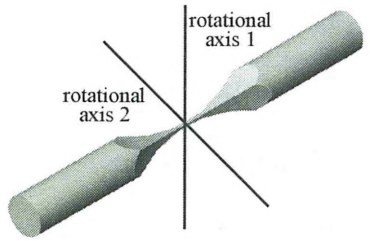

Fig. 6a: Flexure hinge with two DOF

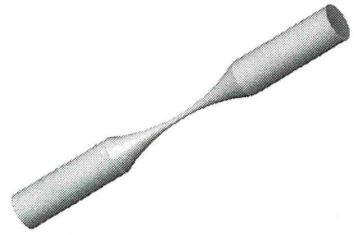

Fig. 6b: Flexure hinge with 3 DOF

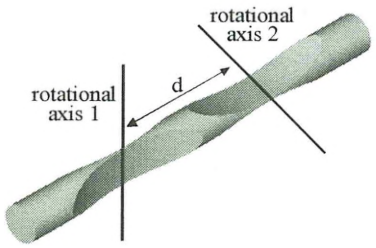

Fig 6c: Flexure hinge with two DOF and non intersecting axes of rotation

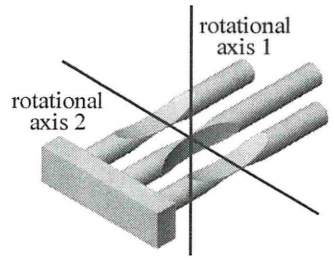

Fig 6d: Combined flexure hinge with two DOF and intersecting axes of rotation

The flexure hinge in figure 6c has two notches perpendicular to each other with an offset of d between the axes of rotation. This hinge is more capable to convey forces but would lead to a modified kinematic behavior of the structure because of the non intersecting rotational axes. For these reasons the flexure hinges with two and three DOF are realized by a combination of flexure hinges with one DOF. Figure 6d shows one of these combinations with two DOF and intersecting rotational axes.

3.2 Compliant structure

Figure 7 shows one sub chain of the structure with integrated flexure hinges. The main geometric parameters, that means the link length d, the angles γ, β and δ (rotation about the linear axis) in the initial position, have not been changed. By this way the formerly used periphery can be shared by the two structures making a comparison between the robots with conventional bearings and flexure hinges easier.

The workspace of the compliant robot is mainly restricted by the limited deflection angle of the flexure hinges. The angles can be computed with the coordinates q_i after solving the IKP. For the inner hinges of the cardan joints this angular deflection is equivalent to the angle $\Delta\delta$, for the outer hinges of the cardan joints (fig. 7b) this angle is $\Delta\gamma$ and for the hinge between the two links the angle is $\Delta\beta$.

The angles can be computed with eq. (6)

$$\Delta\gamma_i = \arccos\left(\frac{q_{i+3} - q_i}{2d}\right) - \gamma_{i,0}, \qquad \Delta\delta_i = \arccos\left(\frac{X_{Ai} - X_{Bi}}{\sqrt{(2d)^2 - (q_{i+3} - q_1)^2}}\right) - \delta_{i,0}, \qquad \Delta\beta_i = 2\Delta\gamma_i. \tag{7}$$

The angles $\gamma_{i,0}$, and $\delta_{i,0}$ are the angles of the initial position of the structure.

The computation of the deflection angles of the hinges replacing the ball joint are more sumptuous. For that purpose a coordinate system has to be formed in the intersecting point of the rotational axes, with the coordinate axes in direction of the rotational axes. The orientation of this system $x_s y_s z_s$ to the global coordinates system XYZ can be described by an orientation matrix $D_{Kardan}(\Psi_s, \theta_s, \varphi_s)$. A suitable chosen vector v, which is fix to the platform and the platform coordinate system x'y'z' respectively, can be described in the hinge coordinates system $x_s y_s z_s$ by

$$v^s = D_{Kardan}(\Psi_s, \theta_s, \varphi_s)^{-1} \cdot D_{Kardan}(\Psi_P, \theta_P, \varphi_P) \cdot v'. \tag{8}$$

To compute the deflections of the hinges the vector v has to be projected to the planes vertical to the rotational axes, this means the planes x_sy_s, x_sz_s and y_sz_s. The angle is then calculable by the scalar product of this projected vector v^s_{proj} and the coordinates axis vertical to the plane. This has to be done for all three chains.

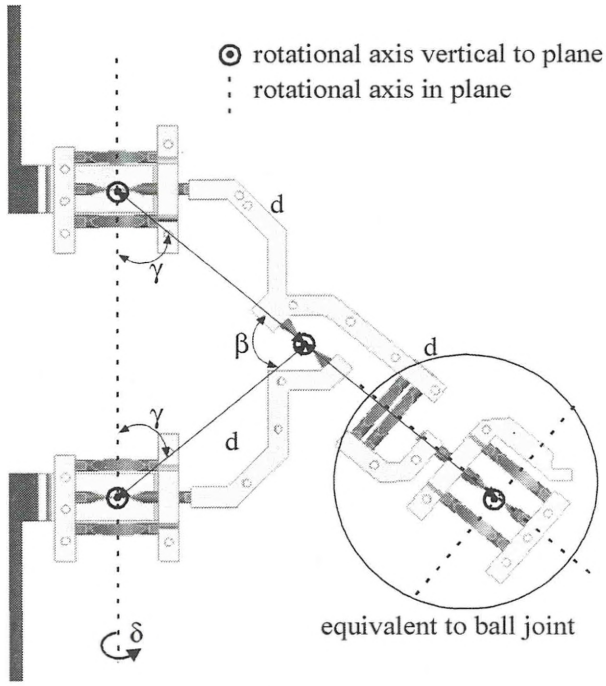

Fig. 7a: One chain of the compliant structure with flexure hinges

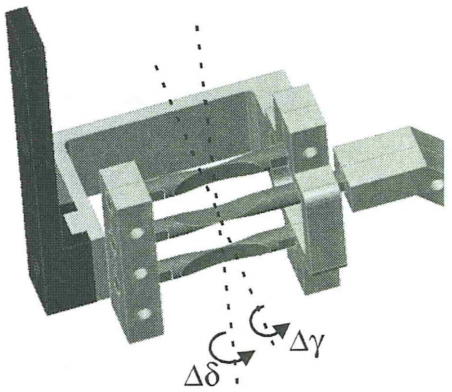

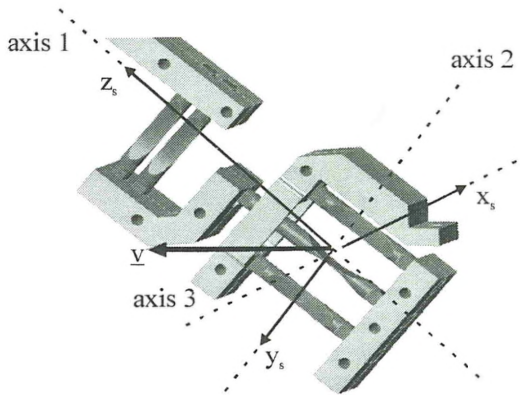

Fig. 7b: Flexible cardan joint with 2 DOF
Fig. 7c: Coordinate system at the hinges composing the ball joint

As a result of this computations we get six angles at each chain which limit the workspace. Restricting the deflection angle of the hinges to 20° the structure has a workspace of 28x28 mm with no additional rotation of the platform (fig. 8).

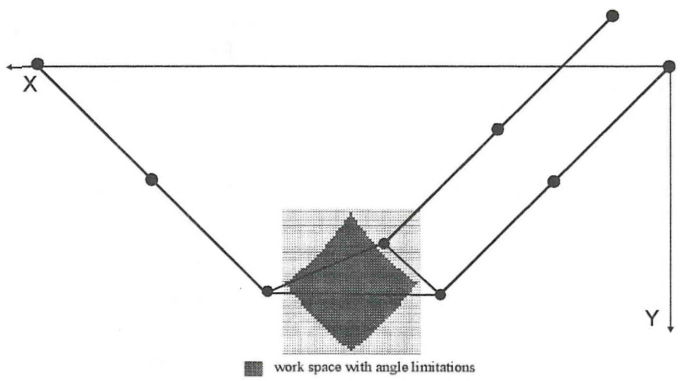

Fig. 8: Workspace of the compliant structure with limitations of the deflections angles of the hinges

A rotation of the platform diminishes the workspace significantly. With an additional rotation of Ψ_P, θ_P , φ_P = 5° the workspace is reduced to ~20x20 mm.

3.3 Outlook

With the help of the FEM it is possible to determine the kinematic deviations between the robot with conventional joints and its ideal kinematic model respectively and the compliant structure with flexure hinges (fig. 9a). Deviations may result from the kinematic behavior of the flexure hinges, unexpected deformations of the assumed rigid parts and unintentional deformations of the hinges, like buckling, due to the real emerging forces and moments in the structure.

For some investigations it is possible to confine the FEM model to one chain, e.g. to detect unintentional deformations of the hinges or the rigid parts. In an optimization the orientation of some hinges, mainly the hinge in point D and the cardan hinges attached to the platform, can be varied to achieve a best possible force and moment transmission into the hinges. The deviations of the compliant structure due to the kinematic deviations between a flexure hinge and an ideal rotational joint have to be investigated with a FEM model of the whole structure.[16]

For this purpose the coordinates of the tool center point $\underline{r}_P = (X_P, Y_P, Z_P, \Psi_P, \theta_P, \varphi_P)$ are varied within the workspace and with the IKP the coordinates q_i of the drives (eq. 5, 6) are computed. These coordinates are then applied as displacement constraints on the parts of the model representing the drives (fig. 9b). With these loads the FEM simulation is solved and the final coordinates of the tool center point of the compliant structure can be determined. The deviations in positioning within the workspace can then be computed to $\Delta r = \sqrt{(X_P - X_{P,M})^2 + (Y_P - Y_{P,M})^2 + (Z_P - Z_{P,M})^2}$, and for the orientation similarly. These deviations only influence the absolute accuracy of the compliant structure. The repeatability will be increased due to the lack of backlash and slip-stick effects in the joints.

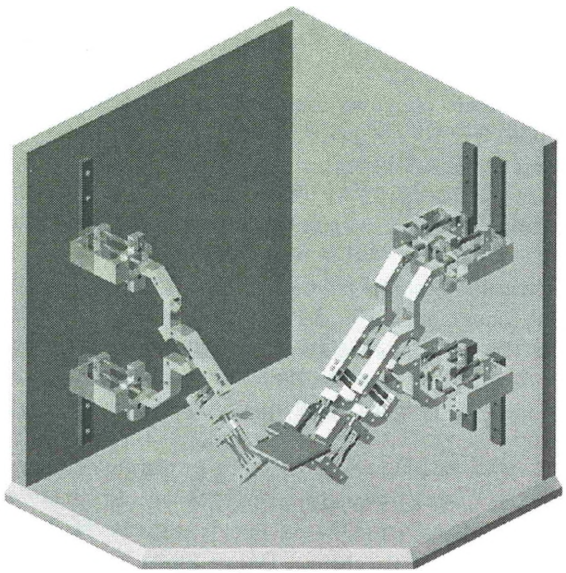

Fig. 9a: Compliant structure with 6 DOF

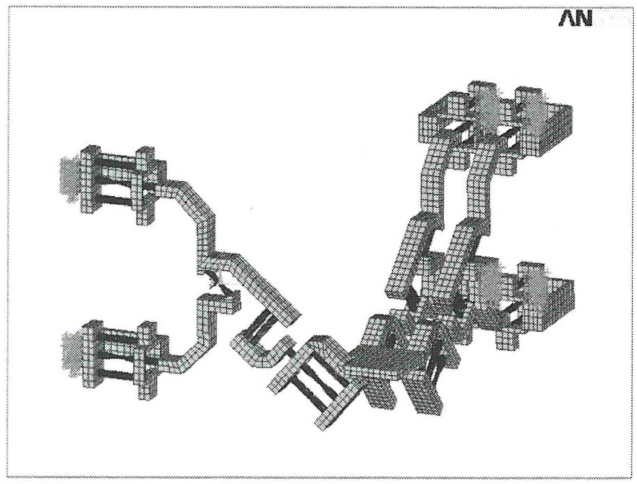

Fig. 9b: Simulation of the kinematic behavior with an FEM model of the structure

4. CONCLUSION

In this paper a compliant parallel structure with six degrees of freedom is presented. The compliant structure has been developed by replacing the conventional bearings by flexure hinges in a previously built parallel robot. The conventional joints with two and three degrees of freedom are substituted by a combination of flexure hinges with only one degree of freedom each. Due to this a kinematic behavior of the compliant structure is achieved, which is similar to that of the structure with conventional bearings. The deviations between the two structures can be simulated with an FEM model of the compliant structure. These FEM simulations will be carried forward as well as repeatability measurements will be done in the near future.

ACKNOWLEDGEMENTS

The authors gratefully acknowledge the financial support by the German Science Foundation (DFG) and Prof. Dr.-Ing. Nicolea Plitea, Visiting Professor from the Technical University Cluj-Napoca, Rumania, for his continuos scientific support.

REFERENCES

1. Patent Nr. D 19710171.2, J. Hesselbach, N. Plitea, H. Kerle, R. Thoben, "Manipulator mit Parallelstruktur", Germany, 2000
2. R. Bierhals, K. Cuhls, V. Hüntrup et. al., "Wirtschaftliche Potentiale der Miniaturisierung aus industrieller Sicht", Studie im Auftrag des Wirtschaftsministeriums Baden-Württemberg, Förderkennzeichen 4-4332.62, 1999
3. S. Bütefisch, S. Büttgenbach, "New differential-type SMA actuator for a miniature silicon gripper", *Proc. of SPIE Smart Materials and MEMS*, SPIE, Melbourne, 2000, in print
4. M. Weck, B. Petersen, "Grippers for the Assembly of Micro Systems in Scanning Electron Microscope", *Production Engineering*, Vol. **V/1**, pp. 67-70, 1998
5. R. Pittschellis, "Mechanische Miniaturgreifer mit Formgedächtnisantrieb", Ph.D. thesis, *Fortschritt-Berichte VDI*, Reihe 8, Nr. **714**, 1998
6. J.-M. Breguet, R. Clavel, "New designs for long range, high resolution, multi-degrees-of-freedom piezoelectric actuators", *Proc. of ACTUATOR '98*, P 28, Messe Bremen GmbH, Bremen, 1998
7. S. Fatikow, U. Rembold, H. Wörn, "Design and control of flexible microrobotics for an automated microassembly desktop-station", *Proc. of SPIE Microrobotics and Microsystem Fabrication*, A. Sulzmann, Vol. **3202**, pp. 66-77, SPIE, Pittsburgh, 1997
8. T. Ebefors, J. U. Mattsson, E. Kälvesten, G. Stemme, "A robust micro conveyer realized by arrayed polimide joint actuators", *J. Micromech. Microeng.*, Vol. **10**, pp. 337-349, 2000
9. U. Gengenbach, J. Boole, "Electrostatic feeder for contactless transport of miniature and microparts", *Proc. of SPIE Microrobotics and Microassembly II*, Nelson, Breguet, Vol. **4194**, pp. 75-81, SPIE, Boston, 2000
10. E. Pernette, S. Henein, I. Magnani, R. Clavel, "Design of parallel robots in microrobotics", *Robotica*, Vol. **15**, pp. 417-420, 1997
11. S. Wang et. al., "Kinematics and force analysis of a 6 d.o.f. parallel mechanism with elastic joints", *Advances in robot Kinematics: Analysis and Control*, Kluver Academic Publishers, pp. 87-96, 1998
12. J. W. Ryu, D. Gweon, K. S. Moon, "Optimal design of a flexure hinge based XYθ wafer stage", *Precision Engineering*, Vol. **21**, pp. 18-28, 1997
13. R. Thoben, "Parallelroboter für die automatisierte Mikromontage", Ph.D. thesis, *Fortschritt-Berichte VDI*, Reihe 8, Nr. **758**, 1999
14. J. Hesselbach, N. Plitea, R. Thoben, "Advanced Technologies for Micro Assembly", *Proc. of SPIE Microrobotics and Microsystem Fabrication*, A. Sulzmann, Vol. **3202**, pp. 178-190, SPIE, Pittsburgh, 1997
15. ANSYS User's Manual, "Vol. IV Theory", ©Swanson Analysis Systems, Inc. 1995
16. J. Hesselbach, A. Raatz, "Pseudo-elastic Flexure-Hinges in Robots for Micro Assembly", *Proc. of SPIE Microrobotics and Microassembly II*, Nelson, Breguet, Vol. **4194**, pp. 157-167, SPIE, Boston, 2000